ELSEVIER

www.elsevier.nl/locate/ica

Inorganica Chimica Acta 300–302 (2000) 992–1003

Inorganica Chimica Acta

Pentadentate thioether-oxime macrocyclic and quasi-macrocyclic complexes of copper(II) and nickel(II)

Michael J. Prushan [a], Anthony W. Addison [a,*], Raymond J. Butcher [b]

[a] *Department of Chemistry, Drexel University, Philadelphia, PA 19104, USA*
[b] *Department of Chemistry Howard University, Washington, DC 20059, USA*

Received 11 December 1999; accepted 17 December 1999

Abstract

A series of new pentadentate thioether-oximes ($TtoxH_2$, $MeTtoxH_2$, $OdtoxH_2$) were synthesized along with their Ni(II) and Cu(II) complexes. BF_2^+-bridging is accomplished by reaction of the H-bonded oxime complex with $BF_3{\cdot}OEt_2$, though when $Cu(BF_4)_2$ is used as the Cu(II) salt, direct macrocyclization occurs during the metal complexation reaction. Crystallographic studies reveal: $[Cu(TtoxH)]ClO_4$ has a N_2S_3 square-pyramidal geometry, with an H-bond forming a quasi-macrocycle. In $[Cu(OdtoxH)](ClO_4){\cdot}[Cu(OdtoxH_2)](ClO_4)_2$, while retaining the same overall geometry as $[Cu(TtoxH)]ClO_4$, half of the cations are singly deprotonated and the remaining half retain both their protons. In addition, there is an unexpected interaction involving a perchlorate oxygen and the dimethylene bridges between the ligand's ether oxygen and thioether sulfurs. $[Ni(OdtoxBF_2)]ClO_4{\cdot}H_2O$ has an $N_2S_2O_2$ octahedral geometry. The ligand occupies the equatorial plane and one of the apical positions; the coordination sphere is completed by a water oxygen. Cyclic voltammetry and rotating disk electrode (RDE) polarography reveal that N_2S_3 donor sets stabilize both Ni(III) and Ni(I), whereas the Cu(II) complexes stabilize only Cu(I). The copper complexes show axial ESR spectra typical of tetragonal Cu(II). Nitrogen superhyperfine structure is observed in both the room temperature fluid and 77 K cryogenic glass spectra. Macrocyclization by BF_2^+ enforces the in-plane geometry around the metal ion.

Keywords: Macrocycle; Crystal structures; Oxime; Copper complexes; Nickel complexes; Electrochemistry; Polarography

1. Introduction

In 1905, Chugaev discovered the vicinal dioxime metal complex bis-dimethylgloximatonickel(II) [1], initiating an area of coordination chemistry which has been widely explored during the past century. The first *vic*-oxime quasi-macrocyclic complexes were prepared by Uhlig and Friedrich [2]. Since that time, several N_4 and N_2S_2 quasi-macrocyclic and BF_2-macrocyclized oximes have been synthesized [3–7]. Recently a copper–oxime complex was used to oxidize anthracene [8], while metal-containing oxime complexes are utilized in medicine as well; technetium(V)- and copper(II)-containing *vic*-oximes currently are used as cerebral and myocardial perfusion imaging agents [9–14]. This area was also recently reviewed [15,16]. The ability of sulfur- and nitrogen-based donors to stabilize reduced and oxidized forms of Cu(II) and Ni(II), respectively, has sparked interest in their role in bioinorganic systems. Interest continues in the combined effects of thioether sulfur with imino nitrogen on the redox chemistry of Cu(II) and Ni(II). We report here the synthesis, structure and electronic properties of Ni(II)- and Cu(II)-oxime complexes with N_2S_3 and N_2S_2O donor arrays, as well as the properties of the BF_2-macrocyclized complexes, some of which exhibit the ability of stabilizing both Ni(I) and Ni(III) in the same ligand framework. It was found that the direct reaction of $Cu(BF_4)_2$ with the dioxime ligands produced the BF_2^+-macrocyclized products.

* Corresponding author. Fax: +1-215-895 1265.
E-mail address: addisona@drexel.edu (A.W. Addison)

0020-1693/00/$ - see front matter
PII: S0020-1693(00)00016-5

2. Experimental

Reagents (Aldrich, Fluka, GFS) were generally used as received. Acetonitrile for electrochemistry was distilled off P_4O_{10} under N_2. 3-Chloro-2-propanone oxime and 3-chlorobutanone oxime were prepared according to literature procedures [7,17]. Proton NMR spectra were obtained on a Bruker AM250 spectrometer using $CDCl_3$ as solvent with TMS as internal standard. Electronic spectra were recorded on a Perkin–Elmer Lambda-3 spectrophotometer (solution) or on a Perkin–Elmer 330 spectrophotometer, equipped with an integrating sphere for diffuse reflectance. Electrochemical measurements were carried out with a Bioanalytical Systems (BAS-100A) electrochemical analyzer. The three-electrode assembly comprised the working electrode, an Ag^+ (0.01 M, 0.1 M NEt_4ClO_4, MeCN)/Ag reference electrode, and a Pt-mesh auxiliary electrode. The working electrode was a Pt wire for voltammetry and a Pt disk for rotating electrode polarography (for which $E_{1/2}$ is defined as the potential at which $i = i_L/2$ [18]. The supporting electrolyte was 0.1–0.2 M NEt_4ClO_4, and solutions were approximately 1 mM in complex. ESR spectra were obtained on a Varian E-12 X-band instrument calibrated near $g = 2$ with diphenylpicrylhydrazyl radical; g-values are ± 0.005 ($g_{\|}$) and ± 0.01 ($g_{\perp}$); isotropic g-values (g_o) are ± 0.005. ESR spectra were simulated (to second order in the resonance fields) on a Macintosh G3 platform using software derived from the work of Lozos et al. [19]. Elemental microanalyses were performed by Robertson–Microlit Laboratories (Madison, NJ) or by the University of Pennsylvania Microanalytical Laboratory. Mass spectra were obtained on a VG-ZABHF high resolution double focusing instrument using 2-nitrobenzyl alcohol as the matrix for FAB mode.

2.1. Syntheses

2.1.1. 4,7,10-Trithiatridecane-2,12-dione dioxime ($TtoxH_2$)

Under an atmosphere of N_2, Na metal (0.69 g, 30 mmol) was dissolved in absolute ethanol (20 ml). Bis(2-mercaptoethyl) sulfide (2.3 g, 15 mmol) was added, followed by $NaBH_4$ (0.33 g, 3 mmol). The mixture was heated to boiling on a steam bath and allowed to cool to room temperature (r.t). An ethanol solution (15 ml) of 3-chloro-2-propanone oxime (3.21 g, 30 mmol) was slowly added with stirring. The mixture was allowed to stir overnight. The ethanol was evaporated off (steam bath) and the residue was partitioned between 20 ml of diethyl ether and 30 ml of water. Three such ether extracts were combined and dried over anhydrous Na_2SO_4. Ether removal (rotary evaporator) afforded a viscous pale yellow oil. Yield: 3.36 g (76%). FAB MS: $M + H = 297$; ^1H NMR: δ 2.0 (s, 6H), 2.7 (m, 8H), 3.3 (s, 4H), 9.9 (s, 2H).

2.1.2. 4,10-Dithia-7-oxatridecane-2,12-dione dioxime ($OdtoxH_2$)

The procedure followed was as above, 2-mercaptoethyl ether (2.07 g, 15 mmol) being used instead of 2-mercaptoethyl sulfide. Yield: 3.90 g (93%). FAB MS: $M + H = 281$; ^1H NMR: δ 2.0 (s, 6H), 2.7 (m, 8H), 3.2 (s, 4H), 3.6 (m, 4H), 9.9 (s, 2H).

2.1.3. 3,11-Dimethyl-4,7,10-trithiatridecane-2,12-dione dioxime ($MeTtoxH_2$)

The procedure followed was as for $TtoxH_2$, but using 3-chlorobutanone oxime (3.63 g, 30 mmol) instead of 3-chloro-2-propanone oxime. Yield: 3.94 g (81%). FAB MS: $M + H = 325$; ^1H NMR: δ 1.4 (2d, 6H), 1.9 (s, 6H), 2.6 (m, 8H), 3.7 (qd, 2H), 9.6 (s, 2H).

The methods for preparation of the Ni(II) and Cu(II) complexes of $TtoxH_2$, $MeTtoxH_2$ and $OdtoxH_2$ were similar. An example of the synthesis is as follows:

2.1.4. $[Ni(TtoxH)]ClO_4 \cdot H_2O$

To a stirred solution of $TtoxH_2$ (2 g, 7.3 mmol) in MeOH (20 ml), was added a solution of $Ni(ClO_4)_2 \cdot 6H_2O$ (2.67 g, 7.3 mmol) in MeOH (10 ml), to give a lilac solution. A methanolic solution (15 ml) of $NaOAc \cdot 3H_2O$ (0.99 g, 7.3 mmol) was then added. After 10 min a powdery lilac precipitate formed, which was filtered off, washed with MeOH (2×5 ml) and recrystallized from hot 2:1 MeOH–Me_2CO. Yield: 1.86 g (52%) of lilac microprisms. *Anal.* Calc. for $C_{10}H_{19}ClN_2NiO_6S_3 \cdot H_2O$: C, 25.2; H, 4.55; N, 5.88. Found: C, 25.2; H, 4.52; N, 5.68%. FAB MS: $(M - ClO_4)^+$: 353.

2.1.5. $[Ni(OdtoxH)]ClO_4 \cdot H_2O$

For 5.0 mmol (1.40 g) of ligand: Yield, 1.33 g (58%) of lilac microprisms. *Anal.* Calc for $C_{10}H_{19}ClN_2NiO_6S_2 \cdot H_2O$: C, 26.4; H, 4.65; N, 6.15. Found: C, 25.4; H, 4.98; N, 6.04%. FAB MS: $(M - ClO_4)^+$: 337.

2.1.6. $[Ni(MeTtoxH)]ClO_4 \cdot H_2O$

For 1 mmol (0.32 g) of ligand: Yield, 0.28 g (56%). Recrystallized from hot 1:3 MeOH–$MeNO_2$ lilac microprisms. *Anal.* Calc for $C_{12}H_{23}ClN_2NiO_6S_3 \cdot H_2O$: C, 29.0; H, 4.66; N, 5.63. Found: C, 28.8; H, 5.14; N, 5.71%. FAB MS: $(M - ClO_4)^+$: 381.

2.1.7. $[Cu(TtoxH)]ClO_4$

For 2 mmol (0.59 g) of ligand: Yield, 0.54 g (59%) (Purple–black solid). Recrystallized from hot 1:1 MeOH–$MeNO_2$ of purple–black single rhombic crystals. *Anal.* Calc for $C_{10}H_{19}Cl \cdot CuN_2O_6S_3$: C, 26.2; H, 4.18; N, 6.11. Found: C, 25.3; H, 4.13; N, 6.00%. FAB MS: $(M - ClO_4 + H)^+$: 359.

2.1.8. [Cu(OdtoxH)](ClO$_4$)·[Cu(OdtoxH$_2$)](ClO$_4$)$_2$

For 2 mmol (0.56 g) of ligand: Yield, 0.84 g (85%). Recrystallized from hot 1:1 MeOH–MeNO$_2$ of purple–black single rhombic crystals. *Anal.* Calc for $C_{10}H_{19.5}Cl_{1.5}CuN_2O_9S_2$: C, 24.4; H, 3.99; N, 5.69. Found: C, 24.5; H, 4.09; N, 5.64%. FAB MS: $(M-ClO_4+H)^+$: 343.

2.1.9. [Cu(MeTtoxH)]ClO$_4$·[Cu(MeTtoxH$_2$)](ClO$_4$)$_2$

For 4.1 mmol (1.35 g) of ligand: Yield, 1.51 g (76%) (purple–black solid). Recrystallized from hot 1:1 MeOH–MeNO$_2$ of purple–black rhombic crystals. *Anal.* Calc. for $C_{12}H_{21.5}Cl_{1.5}CuN_2O_8S_3$: C, 26.8; H, 4.41; N, 5.00. Found: C, 26.9; H, 4.30; N, 4.99%. FAB MS: $(M-ClO_4)^+$: 387.

2.1.10. [Ni(TtoxBF$_2$)]ClO$_4$·0.5CH$_3$OH

To [Ni(TtoxH)]ClO$_4$·H$_2$O (0.472 g, 1.0 mmol) in 20 ml of boiling MeCN, were added 1.0 mmol (0.10 g, 0.138 ml) of triethylamine and 1.0 mmol (0.14 g, 0.125 ml) of boron trifluoride diethyl etherate. The solution was stirred for 1 h at r.t. and the solvent was then evaporated off on a steam bath. The residue was dissolved in 10 ml of water and the resulting lilac solution was cooled by refrigeration for 30 min, after which lilac microcrystalline solid precipitated, which was filtered off, washed with cold H$_2$O (2 × 2 ml) and dried in air. Recrystallization from hot 1:1 MeOH–MeCN (v/v) afforded single lilac prismatic crystals (0.23 g, 44%). *Anal.* Calc for $C_{10}H_{18}BClF_2N_2NiO_6S_3·0.5CH_3OH$: C, 24.4; H, 3.90; N, 5.41. Found: C, 24.3; H, 3.34; N, 5.98%. FAB MS: $M-ClO_4$: 401, $(M-BF_2-ClO_4)^+$: 353.

2.1.11. [Ni(OdtoxBF$_2$)]ClO$_4$·2H$_2$O

A solution of [Ni(OdtoxH)]ClO$_4$·H$_2$O (0.456 g, 1 mmol) was dissolved in MeCN (20 ml), the solution was heated to the boil on a steam bath followed by the addition of triethylamine (0.10 g, 0.138 ml, 1 mmol) and boron trifluoride diethyl etherate (0.14 g, 0.125 ml, 1 mmol). The solution volume was reduced to 10 ml (steam bath), the solution was cooled on ice to precipitate a lilac solid, which was filtered off and washed with MeCN (2 × 3 ml) and Et$_2$O (5 ml) and dried over anhydrous CaCl$_2$ in vacuo. Recrystallized from hot 1:1 MeOH–MeNO$_2$ as lilac microcrystalline prisms. Yield: 0.35 g (70%). *Anal.* Calc. for $C_{10}H_{18}BClF_2N_2NiO_7S_2·2H_2O$: C, 23.0; H, 4.25; N, 5.37. Found: C, 23.9; H, 4.35; N, 5.36%. FAB MS: $(M-ClO_4)^+$: 385.

2.1.12. [Cu(TtoxBF$_2$)]BF$_4$

TtoxH$_2$ (0.7 g, 2.36 mmol) was dissolved in MeOH (20 ml). With stirring, a methanolic solution of Cu(BF$_4$)$_2$ (2.36 mmol) was slowly added to give a dark green solution which immediately precipitated a dark purple solid. The mixture was stirred for 25 min, after which the solution was concentrated down on a steam bath to half the volume. The resulting solid was filtered off, washed with MeOH (3 × 5 ml) and recrystallized from hot MeCN. Yield: 0.40 g (34.3%) of purple rhombic shaped microcrystals. *Anal.* Calc. for $C_{10}H_{18}CuB_2F_6N_2O_2S_3$: C, 24.3; H, 3.68; N, 5.68. Found: C, 24.4; H, 3.46; N, 5.57%. FAB MS: $(M-BF_4)^+$: 406, $(M-BF_2-BF_4)^+$.

2.1.13. [Cu(OdtoxBF$_2$)]BF$_4$·0.5H$_2$O

Same general procedure as above, for 2.0 mmol (0.56 g) of ligand: Yield: 0.15 g (15%) of purple rhombic microcrystals. *Anal.* Calc. for $C_{10}H_{18}B_2CuF_6N_2O_3S_2·0.5H_2O$: C, 24.7; H, 3.94; N, 5.76. Found: C, 24.6; H, 3.67; N, 5.64%. FAB MS: $(M-BF_4)^+$: 390, $(M-BF_2-BF_4)^+$:343.

2.1.14. [Cu(MeTtoxBF$_2$)]BF$_4$

For 1 mmol (0.32 g) of ligand. Recrystallized from hot 1:1 MeOH–Me$_2$CO of purple rhombs. Yield: 0.47 g (91%). *Anal.* Calc. for $C_{12}H_{22}B_2CuF_6N_2O_2S_3$: C, 27.6; H, 4.25; N, 5.37. Found: C, 27.8; H, 4.54; N, 5.41%. FAB MS: $(M-BF_4)^+$: 434, $(M-BF_2-BF_4)^+$: 387.

Caution! *The perchlorate salts used in this study are potentially explosive and should be prepared only in small quantities. [Cu(MeTtoxH)]ClO$_4$ proved to be mechanically sensitive, so due caution in its preparation and handling should be observed.*

2.1.15. X-ray data collection

X-ray data for [Cu(TtoxH)]ClO$_4$ and [Cu(OdtoxH)]-ClO$_4$·[Cu(OdtoxH$_2$)](ClO$_4$)$_2$ were collected on a Siemens P4S diffractometer and refined according to previously published procedures [7].

For [Cu(TtoxH)]ClO$_4$ a total of 1929 reflections were collected ($-7 \le h \le 0$, $-18 \le k \le 0$, $-28 \le l \le 0$) in the range of 2.90 to 27.50°, with all being unique ($R_{int} = 0\%$). The empirically derived transmission coefficient ranged from 0.654 to 0.899. Disorder in the methylene linkages between S1 and S2 was resolved by constraining the bond distances and solving for the relative occupancies which gave the best fit to the diffraction data. The two positions for the methylene carbons have occupancies of 0.732 and 0.268, respectively.

For [Cu(OdtoxH)]ClO$_4$·[Cu(OdtoxH$_2$)](ClO$_4$)$_2$ a total of 2555 reflections were collected ($-18 \le h \le 18$, $-15 \le k \le 0$, $-17 \le l \le 15$) in the range of 2.39 to 28.50°, with 2457 being unique ($R_{int} = 2.15\%$). The empirically derived transmission coefficient ranged from 0.1567 to 0.2961. The labile OdtoxH$_2$ proton is effectively distributed over symmetry-equivalent sites, and thus could not be located in the refinement.

X-ray data for [Ni(OdtoxBF$_2$)]ClO$_4$·2H$_2$O was collected on a Siemens SMART CCD diffractometer sys-

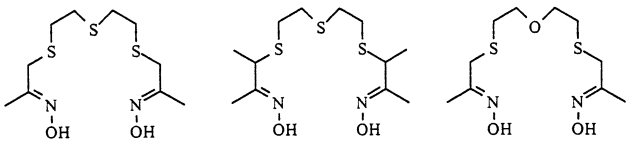

Fig. 1. Ligands treated in this paper.

tem at ambient temperature and data were collected and refined according to previously published procedures [20]. A total of 21404 reflections were collected ($-18 \le h \le 18$, $-11 \le k \le 11$, $-23 \le l \le 23$) in the range of 1.51 to 28.31°, with 4783 being unique (R_{int} = 4.60%). The empirically derived transmission coefficient ranged from 0.4965 to 0.8394. Disorder in the methylene linkages between S(1A) and O, and between S(1B)and O was resolved by constraining the bond distances and solving for the relative occupancies which gave the best fit to the diffraction data. The two almost equivalent positions for the methylene carbons have occupancies of 0.559 and 0.441, respectively. A partially disordered perchlorate was similarly refined by modeling three oxygen sites with 0.292, 0.337, 0.371 occupancies, respectively.

Hydrogens were included in structure factor calculations in calculated positions and refined using a riding model. Thermal ellipsoids are displayed at the 20% probability level for clarity, and hydrogen atoms are shown as spheres of arbitrary size.

3. Results and discussion

Due to their insolubility in methanol, Cu(II) complexes of $OdtoxH_2$ and $MeTtoxH_2$ tend to form compounds that are made up of 1:1 mixtures of non-deprotonated and singly-deprotonated complexes. This insolubility tends to inhibit further deprotonation, which would otherwise lead to the completely quasi-macrocyclized, singly deprotonated products. Attempts to macrocyclize $[Ni(MeTtoxH)]^+$ with BF_2^+ produced only starting material, while attempts to induce reaction of excess $NaBF_4$ with $[Ni(TtoxH)]ClO_4$ in methanol, in order to macrocyclize via a direct reaction with BF_4^- produced only the metathesis product $[Ni(TtoxH)]BF_4$.

3.1. Synthesis of Cu–BF_2^+-macrocyclized oximes

It was found that when $Cu(BF_4)_2$ is used as the Cu^{2+} salt, one is able to obtain in rather good yield, the BF_2^+-macrocyclized *vic*-oxime. It is interesting to note that this reaction does not occur in the case of the Ni(II) oximes, which we attribute to the greater acidity of the copper(II) oxime promoting oximate nucleophile formation. The only other known example of the reaction of BF_4^- with hydrogen-bonded oximes requires the addition of an equimolar amount of $NaBF_4$ to the reaction mixture and refluxing conditions for ~18 h [21]. The reaction described here is a factor of approximately 10^3 times faster and requires neither the addition of excess BF_4^- nor refluxing conditions (Fig. 1, Table 1).

Table 1
Crystallographic data

	$[Cu(TtoxH)]ClO_4$	$[Cu(OdtoxH)]ClO_4 \cdot [Cu(OdtoxH_2)](ClO_4)_2$	$[Ni(OdtoxBF_2)]ClO_4 \cdot 2H_2O$
Empirical formula	$C_{10}H_{19}ClN_2O_6CuS_3$	$C_{10}H_{19.5}Cl_{1.5}N_2O_9CuS_3$	$C_{10}H_{22}BClF_2N_2NiO_9S_2$
Formula weight	458.44	524.70	521.39
Crystal system	orthorhombic	monoclinic	monoclinic
Crystal size (mm)	$0.06 \times 0.47 \times 0.17$	$0.30 \times 0.88 \times 0.50$	$0.1 \times 0.36 \times 0.36$
Space group	*Pbcm*	*C*2/*m*	$P2_1/c$
a (Å)	5.4075(17)	13.877(2)	13.7476(10)
b (Å)	14.043(4)	11.448(2)	8.3275(6)
c (Å)	21.650(6)	12.693(2)	17.4205(12)
β (°)	90	113.376(14)	100.6690(10)
V (Å^3)	1644.0(8)	1850.9(6)	1959.9(2)
Z	4	4	4
ρ_{calc} (g cm^{-3})	1.852	1.833	1.767
F(000)	940	1004	1072
μ (mm^{-1})	1.901	1.668	1.405
λ (Mo Kα) (Å)	0.71073	0.71073	0.71073
T (K)	293(2)	293(2)	223(2)
R [a], R_w [b]	0.0426; 0.0837	0.0529; 0.1386	0.0523; 0.1476

[a] $R = \Sigma||F_o|-|F_c||/\Sigma|F_o|$.
[b] $R_w = [\Sigma w(|F_o|-|F_c|)^2/\Sigma w(F_o)^2]^{1/2}$.

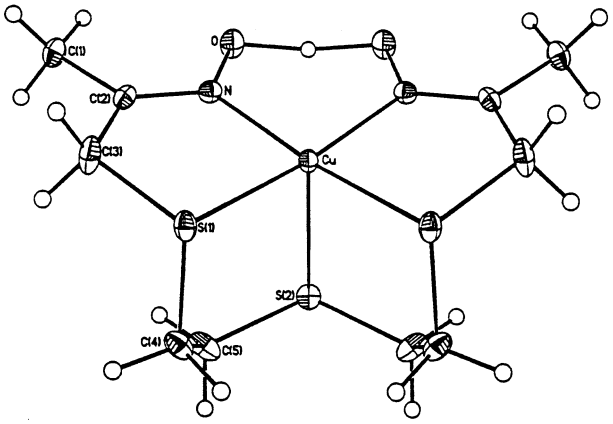

Fig. 2. ORTEP projection of the $[Cu(TtoxH)]^+$ cation in $[Cu(TtoxH)]ClO_4$.

Table 2
Selected bond lengths (Å) [a] and angles (°) [a] for $[Cu(TtoxH)]ClO_4$

Cu–N	2.001(3)	N–O	1.361(4)
Cu–S(1)	2.3353(12)	(1)–C(3)	1.797(4)
Cu–S(2)	2.4822(18)	S(1)–C(4)	1.789(6)
N–C(2)	1.284(5)	S(2)–C(5)	1.836(6)
N–Cu–S(1)	84.23(10)	N–C(2)–C(3)	118.4(4)
N–Cu–S(2)	101.02(10)	C(2)–C(3)–S(1)	115.1(3)
S(1)–Cu–S(2)	90.40(5)	C(4)–C(5)–S(2)	116.3(5)
O–N–Cu	118.8(2)	C(2)–N–O	117.1(3)
C(2)–N–Cu	123.9(3)	N–C(2)–C(1)	124.8(4)
C(5)–S(2)–Cu	96.6(2)		

[a] Parentheses contain estimated standard deviation in the least significant digit.

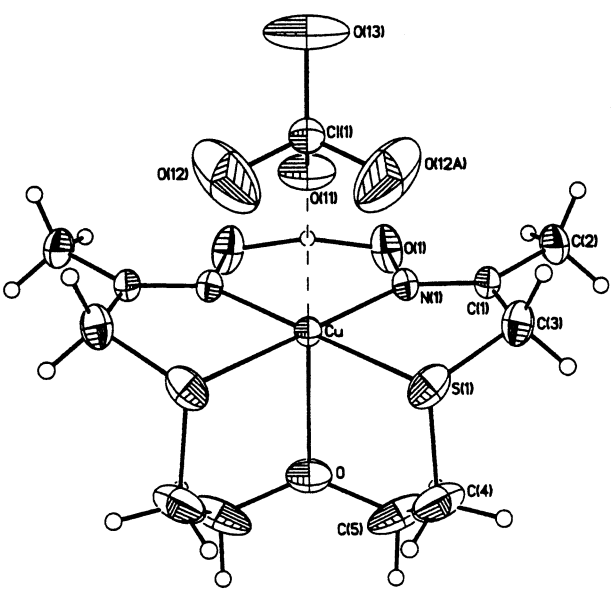

Fig. 3. ORTEP projection of $[Cu(OdtoxH)]ClO_4$ in $[Cu(OdtoxH)](ClO_4)\cdot[Cu(OdtoxH_2)](ClO_4)_2$.

3.2. Description of the structure of $[Cu(TtoxH)]ClO_4$

An ORTEP projection is shown in Fig. 2, while selected bond distances and angles are given in Table 2. The X-ray structure reveals an almost perfect square pyramidal N_2S_3 coordination environment ($\tau = 0.06$) [22]. The Cu(II) in each quasi-macrocyclic unit is coordinated by two *cis*-thioether sulfur and two *cis*-oxime nitrogen donors in the basal plane and by the ligand's central thioether sulfur in the apical position. The equatorial Cu–S (2.335 Å) distances are identical to that of the only other structurally characterized thioether–oxime complex of Cu(II) (2.33 Å) in the literature [23]. The Cu–N(oxime) (2.00 Å) distances are typical for compounds of this nature [24–26]. A single proton bridging the two oxime oxygens closes off the equatorial chelate ring, which is typical for metal complexes with two oximes in a *cis*-conformation. The O···O′ separation (2.429 Å) is consistent with H-bonded oxime O···O′ distances found in other *vic*-dioxime complexes [6,27]. The axial Cu–S distance (2.482 Å) is considerably longer than those in the equatorial plane, but typical for Jahn–Teller elongated axial thioether donors [28].

3.3. Description of the structure of $[Cu(OdtoxH)](ClO_4)\cdot[Cu(OdtoxH_2)](ClO_4)_2$

An ORTEP projection is shown in Fig. 3 and a representation of the unit cell, showing the intramolecular interactions is shown in Fig. 4; selected bond distances and angles are in Table 3. The X-ray structure reveals a square pyramidal N_2S_2O coordination environment ($\tau = 0.07$), the overall coordination mode be-

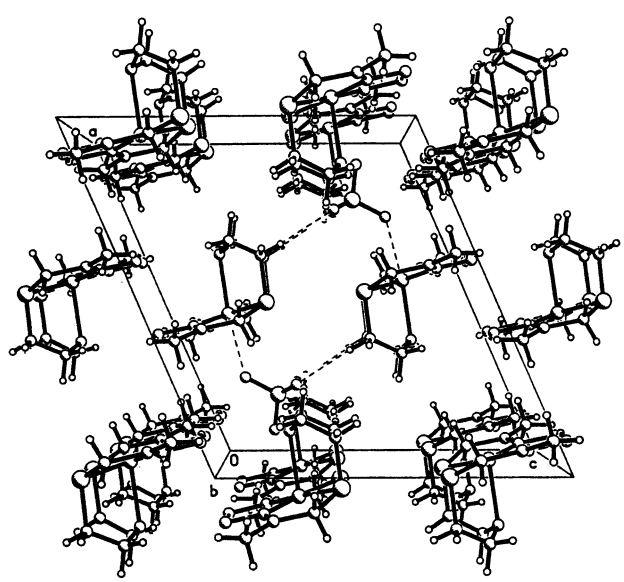

Fig. 4. *ab* Projection of the unit cell for $[Cu(OdtoxH)](ClO_4)\cdot[Cu(OdtoxH_2)](ClO_4)_2$ showing the tetramolecular cluster involving two bridging perchlorates and two $[Cu(OdtoxH)]^+$ cations.

Table 3
Selected bond lengths (Å) [a] and angles (°) [a] for [Cu(OdtoxH)]-(ClO_4)·[Cu(OdtoxH_2)]$(ClO_4)_2$

Cu–N(1)	1.979(3)	N(1)–O(1)	1.391(4)
Cu–S(1)	2.3180(12)	S(1)–C(3)	1.774(7)
Cu–O	2.316(5)	S(1)–C(4)	1.772(7)
N(1)–C(1)	1.273(5)	O–C(5)	1.485(9)
N(1)–Cu–S(1)	83.54(10)	N(1)–C(1)–C(2)	125.1(5)
N(1)–Cu–O	97.65(13)	N(1)–C(1)–C(3)	116.9(4)
S(1)–Cu–O	84.18(10)	C(5)–C(4)–S(1)	117.1(5)
O–N(1)–Cu	120.9(2)	C(5)–O–Cu	106.1(4)
C(1)–N(1)–Cu	124.9(3)	C(1)–C(3)–S(1)	115.6(3)
C(4)–S(1)–Cu	100.5(3)		

[a] Parentheses contain estimated standard deviation in the least significant digit.

Table 4
Selected bond lengths (Å) [a] and angles (°) [a] for [Ni(OdtoxBF_2)]-ClO_4·2H_2O

Ni–S(1A)	2.4018(11)	N(1A)–O(1A)	1.398(4)
Ni–S(1B)	2.3995(10)	N(1B)–O(1B)	1.389(4)
Ni–O	2.126(3)	N(1A)–C(2A)	1.280(4)
Ni–O(1W)	2.044(3)	N(1B)–C(2B)	1.288(4)
Ni–N(1A)	2.045(3)	C(3A)–S(1A)	1.808(6)
Ni–N(1B)	2.034(3)	C(3B)–S(1B)	1.804(5)
O(1A)–B	1.475(5)	C(5C)–O	1.463(6)
O(1B)–B	1.460(5)	C(5D)–O	1.445(6)
S(1A)–Ni–S(1B)	99.12(4)	N(1A)–Ni–N(1B)	94.43(11)
S(1A)–Ni–O	83.58(7)	O(1A)–N(1A)–Ni	122.7(2)
S(1B)–Ni–O	83.94(8)	O(1B)–N(1B)–Ni	121.3(2)
S(1B)–Ni–N(1B)	83.30(8)	C(2A)–N(1A)–O(1A)	113.6(3)
N(1B)–Ni–O(1W)	93.02(13)	C(2B)–N(1B)–O(!B)	113.7(3)
O(1W)–Ni–O	171.01(13)		

[a] Parentheses contain estimated standard deviation in the least significant digit.

ing similar to that of [Cu(TtoxH)]ClO_4. The oxime H-bonded O···O′ distance is 2.530 Å and is again comparable with other *vic*-oxime oxygen distances (vide supra). The equatorial Cu–S (2.318 Å) and Cu–N (1.979 Å) distances are slightly smaller compared with [Cu(TtoxH)]ClO_4, probably due to the smaller size of the ether oxygen donor allowing the ligand to be brought closer to the metal. The axial Cu–O (2.316 Å) distance is also typical for elongatedly axial oxygen donors [29]. The unit cell contents (as well as the other experimental evidence) indicate that half of the complex cations are in the $[Cu(OdtoxH)]^+$ form, and the other half in the $[Cu(Odtox H_2)]^{2+}$ form. The additional (second) proton in the latter formula is disordered over the four oxime oxygens of the two formula units. A perchlorate O(11) is located directly above each CuN_2S_2 plane, weakly bound at 2.524 Å from the copper(II).

In addition, there is an unexpected interaction involving a perchlorate oxygen and the dimethylene bridges between the ligand's ether oxygen and thioether sulfurs. The 2 equiv. perchlorate O(12) act as H-bond acceptors with respect to the two methylene protons of the C(4) atoms adjacent to the thioether sulfurs. The two C–H groups are directed toward the two O's, the H···O distance being 2.463 Å and the C–H···O angle 160.6°. H-bonding interactions involving hydrocarbons are not so common, but the distances are in the range of 2.4–3.0 Å [30–33]. Consequently, there exist tetramolecular clusters involving two bridging perchlorates and two complex cations, linked in a cyclic structure by two Cu···$OClO_3$ interactions and two pairs of C–H···$OClO_3$ hydrogen bonds.

3.4. Description of the structure of [Ni(OdtoxBF_2)]ClO_4·2H_2O

An ORTEP projection is shown in Fig. 5, with selected bond distances and angles given in Table 4. The macrocyclic structure shows a distorted octahedral geometry around Ni(II), with each Ni(II) coordinated by two *cis*-thioether sulfur and two *cis*-oxime nitrogen donors, and by the ether oxygen in an axial position. The overall disposition of the ligand around the nickel is the same as the above described Cu(II) complexes. The remaining apical site in the octahedral coordination sphere is occupied by a water oxygen. The ligand is macrocyclized by the BF_2^+ group, which bridges the two *cis*-oxime oxygens. The equatorial Ni–S (2.402, 2.400 Å) distances are longer by ~0.24 Å and the Ni–N (2.045, 2.034 Å) distance are ~0.14 Å longer compared to those found in [Ni(Dtdo)]ClO_4, but are quite similar to those found in [Ni_3(Dtox)(OdtoxH_2)]-$(ClO_4)_2$·CH_3CN [6,7]. The oxime O–B bond lengths (1.475, 1.460 Å) are comparable with those found in molecules such as [Ni(Cyclops)I] [34], while the axial ether O–Ni distance (2.126 Å) is slightly larger than the axial water O–Ni distance (2.044 Å).

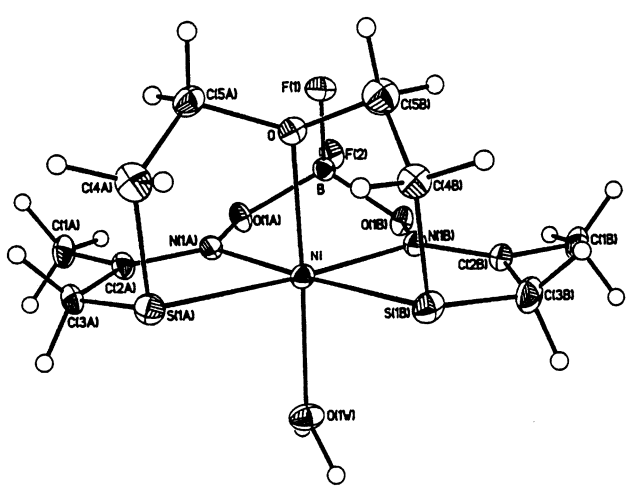

Fig. 5. ORTEP projection of the $[Ni(OdtoxBF_2)]^+$ cation in [Ni(OdtoxBF_2)]ClO_4.

Table 5
Electronic absorption spectra

Complex	Medium [a,c]	λ (nm) (ε (M^{-1} cm^{-1}))	10 Dq [d] (cm^{-1})
$[Ni(TtoxH)]ClO_4 \cdot 1.2H_2O$ [b]	CH_3CN	991 sh (15), 870 (26), 515 (24)	11943
	solid state	955 sh, 880, 540	
$[Ni(TtoxBF_2)]ClO_4 \cdot 0.5CH_3OH$	CH_3CN	971 sh (18), 868 (30), 520 (23)	11832
	CH_3NO_2	964 sh (24), 895 (30), 528 (20)	11037
	solid state	935 sh, 900, 545	
$[Ni(OdtoxH)]ClO_4 \cdot H_2O$	CH_3CN	985 (6.9), 874 (6.8), 740 (10), 539 (28)	11546
	CH_3NO_2	963 sh (18), 838 (22), 549 (44)	10972
	solid state	1000 sh,770, 555	
$[Ni(OdtoxBF_2)]ClO_4 \cdot H_2O$	CH_3CN	984 (7.7), 861 (8.0), 792 (8.1), 542 (17)	10951
	CH_3NO_2	1038 (7.2), 855 (6.4), 788 (6.6), 552 (18)	10416
	solid state	1035, 775,560	
$[Ni(MeTtoxH)]ClO_4 \cdot H_2O$	CH_3CN	1002 (13), 862 (30), 512 (27)	13002
	CH_3NO_2	978 sh (12), 834 (26), 528 (23)	13525
	solid state	960 sh, 855, 540	
$[Cu(TtoxH)]ClO_4$	CH_3CN	906 (79), 550 (458), 419 (345), 341 (562)	
	CH_3NO_2	882 (84), 551 (532), 399 (1781)	
	DMF	814 sh (40), 550 sh (228), 429 (993), 332 (1375)	
	solid state	945, 570, 380 sh	
$[Cu(TtoxBF_2)]BF_4$	CH_3CN	878 (115), 565 (373.0), 346 (1084)	
	CH_3NO_2	882 (130), 563 (438), 394 (1885)	
	DMF	883 (77), 572 (221), 347 (2303)	
	solid state	960, 600, 370 sh	
$\{[Cu(OdtoxH)](ClO_4) \cdot [Cu(OdtoxH_2)](ClO_4)_2\}$	CH_3CN	605 (553), 424 (555), 373 (942), 329 (1079)	
	CH_3NO_2	570 (334), 415 (1075)	
	DMF	819 sh (66), 568 (232), 419 sh (631), 339 (1202)	
	solid state	700 sh, 570, 370 sh	
$[Cu(OdtoxBF_2)]BF_4 \cdot 0.5H_2O$	CH_3CN	572 (187), 342 (1374)	
	CH_3NO_2	743 sh (89), 569 (234), 394 (1310)	
	DMF	797 (42), 588 (141.3), 342 (3605)	
	solid state	700 sh, 570, 350 sh	
$\{[Cu(MeTtoxH)](ClO_4) \cdot [Cu(MeTtoxH_2)](ClO_4)_2\}$	CH_3CN	908 (203), 547 (1167), 429 (825), 344 (1570)	
	CH_3NO_2	890 (111), 550 sh (724), 414 (2023)	
	DMF	789 (107), 556 sh (685), 424 (1093), 330 (1538)	
	solid state	940, 656, 380 sh	
$[Cu(MeTtoxBF_2)]BF_4$	CH_3CN	865 (122), 570 (309), 349 (1120)	
	CH_3NO_2	863 (190), 570 (325), 392 (1907)	
	DMF	874 (84), 572 (208), 348 (1723)	
	solid state	910, 570, 370	
$Cu(CF_3SO_3)_2$	DMF	809 (30), 265 (2553)	

[a] Solid-state data from diffuse reflectance in $MgCO_3$ matrix.
[b] Insoluble in $MeNO_2$
[c] ν_2 values in nickel solid state spectra are obscured by instrument artifacts.
[d] 10 Dq values for solution spectra were calculated according to Hancock's method [32].

3.5. Electronic spectra

The spectroscopic data are summarized in Table 5.

3.5.1. Nickel(II) complexes

Three d–d transitions are generally observed for hexacoordinate Ni(II) ($^3T_{2g} \leftarrow {}^3A_{2g}$, $^3T_{1g}(F) \leftarrow {}^3A_{2g}$, and $^3T_{1g}(P) \leftarrow {}^3A_{2g}$). With donor atoms from row-3 and beyond, the Ni(II) spectra become less straightforward to interpret. Generally, it is known that only two d–d transitions are observed when thioether donors are present, the highest energy band ($^3T_{1g}(P) \leftarrow {}^3A_{2g}$) becoming obscured by the charge-transfer processes ($\sim$400 nm) [35]. Two other problems are often encountered in Ni(II)–thioether and nitrogen containing systems which are interrelated: (a) The mathematical relation-

ships involving spectral transitions and the ligand field parameters break down if there are row-3 donors in the coordination sphere [36]; (b) the lowest energy band ($^3T_{2g} \leftarrow {}^3A_{2g}$) often exhibits a double-humped shape due to mixing with a close-lying spin-forbidden transition ($^1E_g \leftarrow {}^3A_{2g}$) through spin-orbit coupling [37,38]. These problems make it difficult to obtain values for 10 Dq as well as Hancock and coworkers have attempted to tackle the problem of determining 10 Dq by 'deconvoluting' the low energy spin-allowed (10 Dq) from the spin-forbidden transition and the method has been used to interpret the spectra of other hexacoordinate Ni(II) systems with thioether and nitrogen donors [36,39]. In the nickel complexes discussed in this study, only the first two d–d transitions (ν_1, ν_2) are observed. The transition ν_1 is split into a double-humped peak, which can be interpreted as indicated above, but attempts to calculate the Racah B parameter produced values which were physically unrealistic for those reasons. The values obtained for 10 Dq (10 400–13 500 cm^{-1}) are reasonable for pseudo-octahedral high-spin Ni(II) complexes with strong in-plane fields [7,40,41]. The values of 10 Dq are larger for those compounds which possess an axial thioether relative to those with ether axial donors. This difference is due to the larger ligand field strength of thioether donors compared to ether donors [38].

3.5.2. Copper(II) complexes

Optical spectral data for the Cu(II) complexes are given in Table 5. The spectra are generally consistent with Cu(II) with *N*,*S*-coordination. The complexes exhibit two ligand-field bands. For those compounds with axial sulfur donors, one ligand-field band is centered around 570 nm, and the other, less intense band around 890 nm on average. Replacing the axial S(thioether) by O(ether) shifts the ligand field bands to around 418–600 nm. This shift is consistent with a lower ligand field induced by oxygen donors compared to sulfur donors, within a pentacoordinate Cu(II) complex with strongly interacting in-plane donors [40]. The bands between 329 and 429 nm are due to S → Cu(II) charge transfer [42,43].

Two sulfur LMCT bands are observed in the complexes where a proton resides on one or both oximes (in CH_3CN or DMF only), whereas in the BF_2^+ macrocycles, only one sulfur LMCT band is evident. Aoi et al. noted that acetonitrile or DMF coordination tends to shift charge transfer bands to longer wavelengths [44]. ESR evidence also supports the conclusion that solvents may displace endogenous ligand donors from their positions as seen in the solid state structure (vide infra).

3.6. Electrochemistry

A synopsis of the electrochemical data is given in Table 6 (Fig. 5). Fig. 6 shows a cyclic voltammo-

Table 6
Electrochemical data for the complexes in CH_3CN solution

Complex [b]	$E_{1/2}$ (V) [a]		$E_{1/2}$ (V) [a]		10^8 $D\eta$ [e]
	M(II)–M(I)	i_{pa}/i_{pc}	M(II)–M(III)	i_{pc}/i_{pa}	
[Ni(TtoxH)]ClO_4·1.2H_2O [f]	−1.20	0.918	+0.72	0.70	1.82 [h], 2.70 [i]
[Ni(TtoxBF$_2$)]ClO_4·0.5CH_3OH [f]	−1.09	0.71	+1.11	0.82	1.15 [h], 0.66 [i]
[Ni(OdtoxH)]ClO_4·H_2O [f]	−1.27	0.84			1.20 [h]
[Ni(OdtoxBF$_2$)]ClO_4·H_2O [f]	−1.07	0.84			1.31 [h]
[Ni(MeTtoxH)]ClO_4·H_2O [f]	−1.17	0.96	+0.71	0.70	1.65 [h], 2.04 [i]
[Cu(TtoxH)]ClO_4 [g]	−1.10				2.23 [h]
[Cu(TtoxBF$_2$)]BF_4 [d,f]	−0.15	0.62			0.94 [h]
{[Cu(OdtoxH)](ClO_4)·[Cu(OdtoxH$_2$)]$(ClO_4)_2$} [c,d,g]	−1.15				3.31 [h]
[Cu(OdtoxBF$_2$)]BF_4·0.5H_2O [d,g]	−0.22				1.56 [h]
{[Cu(MeTtoxH)](ClO_4)·[Cu(MeTtoxH$_2$)]$(ClO_4)_2$} [c,d,g]	−0.90				1.92 [h]
[Cu(MeTtoxBF$_2$)]BF_4 [f]	−0.17	0.82			1.63 [h]

[a] $E_{1/2}$ vs. Ag^+ (0.01 M, 0.1 M NEt_4ClO_4, CH_3CN)/Ag with Pt electrode. This electrode is at approximately +0.540 V vs. the SHE [45].
[b] 0.1 M NEt_4ClO_4 supporting electrolyte. All electrochemistry was performed in CH_3CN.
[c] Required addition of 1 equiv. triethylamine to observe Cu(II) → Cu(I) reduction for singly deprotonated form. Half singly-deprotonated forms show irreversible redox processes at: +0.20 V for {[Cu(OdtoxH)](ClO_4)·[Cu(OdtoxH$_2$)]$(ClO_4)_2$}, and +0.33 V for {[Cu(MeTtoxH)](ClO_4)·[Cu(MeTtoxH$_2$)]$(ClO_4)_2$}.
[d] Cu(I) is generally unstable and is rapidly converted to Cu(0): [Cu(TtoxBF$_2$)]BF_4 $E_{1/2}$ ca. −0.93 V; {[Cu(OdtoxH)](ClO_4)·[Cu(OdtoxH$_2$)]$(ClO_4)_2$} $E_{1/2}$ ca. −1.8 V; [Cu(OdtoxBF$_2$)]BF_4·0.5H_2O $E_{1/2}$ ca. −1.3 V; {[Cu(MeTtoxH)](ClO_4)·[Cu(MeTtoxH$_2$)]$(ClO_4)_2$} $E_{1/2}$ ca. −1.8 V from RDE polarogram.
[e] $D\eta$ in g cm s^{-2}; η(1 M TEAP in CH_3CN) = 0.00380 g cm^{-1} s^{-1}.
[f] Not adjusted for α, Ψ [46].
[g] $E_{1/2}$ and $D\eta$ obtained from RDE polarogram, estimate of $D\eta$ obtained according to Levich [47] and Adams [48].
[h] For M(II) → M(I).
[i] For M(II) → M(III).

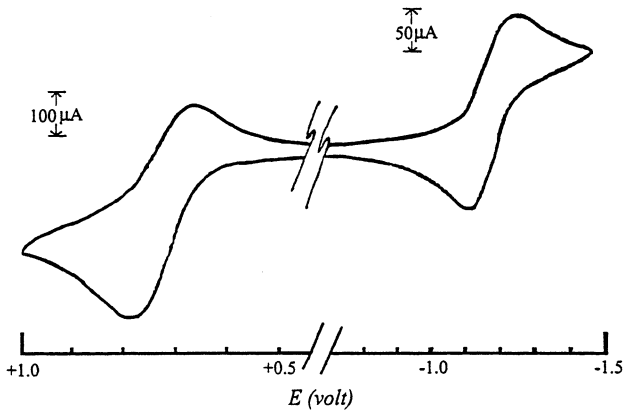

Fig. 6. Cyclic voltammogram of $[Ni(TtoxH)]ClO_4 \cdot H_2O$ in MeCN–NBu_4PF_6 showing both the reduction and oxidation waves. The reductive wave is at a 100 mV s^{-1} scan rate and the oxidative wave at 1000 mV s^{-1} scan rate. Potential scale referred to the Ag^+/Ag electrode.

gram with both the oxidation and reduction for $[Ni(TtoxH_2)]ClO_4 \cdot H_2O$. Many oxime-containing ligands stabilize Ni(III), and Ni(IV) as well as Cu(III), which usually have six donor atoms in the case of nickel and four in the case of copper [49–55]. Here we looked at the redox properties of Ni(II) and Cu(II) complexes with ligands that have five donors. These combine the effects of (i) imino oxime nitrogen donors with (ii) thioether sulfurs and (iii) either H-bond oxime quasi-macrocyclization or covalent macrocyclization (with BF_2^+). It is generally observed that for Ni(II)/Ni(I) redox couples, larger numbers of thioether donors tend to relatively stabilize the formation of Ni(I) [7,56–58], whereas larger numbers of imino-nitrogen donors tend to stabilize Ni(III) [58,59]. Higher oxidation states of nickel are commonly accessible in systems with oximato-nitrogen donors, as a result of the coulombic influence of the negative charge on the HOMO energy [60] and of σ-donation effects [52].

In both the copper and nickel complexes, the BF_2^+-macrocyclized complexes are reduced more readily than the H-bonded, which is directly related to the electron withdrawing ability of BF_2^+ relative to H^+. This effect is an order of magnitude larger in the case of the copper complexes, presumably due to the combination of the inductive effect with structural factors associated with replacing H^+ by BF_2^+. The redox chemistry of the nickel complexes reveals that the ligands presented in this paper are capable of stabilizing both Ni(I) and Ni(III) due to the simultaneous influences of three thioether sulfur donors and the anionic nature of the ligand. Generally the reduction and oxidation waves are quasi-reversible (i_{pa}/i_{pc} approaches unity only at scan rates >300 mV s^{-1}), likely as a result of carbon–sulfur bond cleavage, at least in the oxidized species, and coordinative instability of the Cu(I) species. The stabilization of both Ni(I) and Ni(III) by the same ligand is quite uncommon. Studies of Ni(II) complexes for which reversible or quasi-reversible Ni^{3+}/Ni^{2+}, and Ni^{+2}/Ni^+ couples are observed commonly show differences between these two waves ($E_{oxid} - E_{red}$) varying from 1.8 to 2.6 V [39,40,61–63]. In the nickel complexes reported here only those with three thioether donors show both Ni^{3+}/Ni^{2+} and Ni^{+2}/Ni^+ processes. The differences between the oxidation and reduction waves vary from 1.88 V for $[Ni(MeTtoxH)]ClO_4 \cdot H_2O$ (1.92 V for $[Ni(TtoxH)]ClO_4 \cdot H_2O$) to 2.2 V for $[Ni(TtoxBF_2)]ClO_4 \cdot 0.5CH_3OH$.

The copper complexes exhibit only a reduction wave, at quite negative (the H-bonded oximes) to slightly negative potentials (BF_2^+-bridged oximes). Most of the reductions are irreversible, as the Cu(I) forms are unstable toward conversion to Cu(0) which tends to plate out on the electrode surface. Those complexes which exhibit quasi-reversible reductions both have three thioether donors and also are macrocyclized by BF_2^+ ($[Cu(TtoxBF_2)]BF_4$ and $[Cu(MeTtoxBF_2)]BF_4$). The effect of the BF_2^+ bridge is fairly constant for all of the compounds: replacing the oxime-H by BF_2^+ stabilizes Cu(I) by about 700–900 mV relative to oxime-H. This effect is unexpectedly large compared with what has previously been observed for $[Cu(PreH)]^+$ and $[Cu(cyclops)]^+$ [3] possibly due to the combined structural and electronic effect of thioether donors and the electron withdrawing ability of the BF_2^+.

3.7. Electron spin resonance

The EPR spin-Hamiltonian parameters for the copper(II) complexes are given in Table 7. An example of the ambient temperature and 77 K solution spectra are given in Fig. 7. The EPR parameters, particularly the $A_\parallel$ and $g_\parallel$-values of the Cu(II) complexes, are notably similar to each other and rather independent of axial donor type. As these values are controlled principally by the equatorial plane donors, this indicates a commonality in the detailed equatorial stereochemistry as well as of equatorial donor type. All the values of $g_\parallel > g_\perp$ indicate a $d_{x^2-y^2}$ ground state, which is typical for tetragonal copper complexes. As a result of the strong equatorial donor dominance, the complexes exhibit axial spectra in all but one case (solid state spectrum of $[Cu(TtoxBF_2)]BF_4$). It has been advanced that interpretability in terms of structure is vitiated by exchange interactions when axial spectra with $g_{min} > 2.04$ are observed, this is particularly so when $G < 4$ [64,65]. However, within the limits of our data analyses (including simulations) these sulfur-containing coordination spheres frequently elicit G-values ranging from 2.04 to 4.2 even in solution, so we conclude that exchange interations are not necessarily obscurative for the neat powders of these compounds unless $G < 2.04$

Table 7
Electron spin resonance data

Complex	Medium [a]	g_o [c]	$10^4 \times \lvert A_o \rvert$ [b] (cm^{-1}) [c]	$10^4 \times \lvert A_o(N) \rvert$ (cm^{-1}) [c]	$g_\parallel$ [c]	$10^4 \times \lvert A_\parallel \rvert$ (cm^{-1}) [d]	$g_\perp$ [c]	$10^4 \times \lvert A_\perp \rvert$ (cm^{-1}) [c]	$10^4 \times \lvert A_o(N) \rvert$ (cm^{-1}) [c]
$[Cu(TtoxH)]ClO_4$	DMF	2.050	77	12	2.163	200 [b]	2.08	16 [b]	18
	solid				2.17		2.05		
$[Cu(TtoxBF_2)]BF_4$	DMF	2.057	77	[d]	2.167	212 [b]	2.06	9 [b]	[d]
	solid				$g_3 = 2.12$	$g_1 = 2.04$	$g_2 = 2.07$		
$[Cu(OdtoxH)](ClO_4)\cdot[Cu(OdtoxH_2)](ClO_4)_2$	DMF	2.060	80	11	2.170	219 [b]	2.07	10 [b]	18
	solid				2.17		2.05		
$[Cu(OdtoxBF_2)]BF_4\cdot 0.5H_2O$	DMF	2.074	77	[d]	2.210	232 [b]	2.07	6	18
	solid								
$[Cu(MeTtoxH)](ClO_4)\cdot[MeTtoxH_2)](ClO_4)_2$	DMF	2.055	77	15	2.196	155 [b]	2.08	8 [b]	20
	solid				2.21		2.05		
$[Cu(MeTtoxBF_2)]BF_4$	DMF	2.057	80	17	2.165	208 [b]	2.06	16 [b]	15
	solid				2.16		2.05		

[a] 10% BuOH–DMF was used as solvent for ambient-T isotropic as well as 77 K cryogenic spectra (spectra were identical in pure DMF, but the addition of 10% BuOH provided superior glassing properties). Solid state spectra were obtained from neat powders at 77 K.
[b] Copper hyperfine coupling parameter.
[c] g_o, A_o from RT fluid spectra; $g_\parallel$, $A_\parallel$, $g_\perp$ from 77 K, $g_\perp$ value obtained via simulation; $A_\perp$ via $3A_o = A_\parallel + 2A_\perp$. g_o, $g_\parallel \pm 0.005$; 10^4 $A \pm 3$; $g_\perp \pm 0.01$.
[d] No N-shf observed.

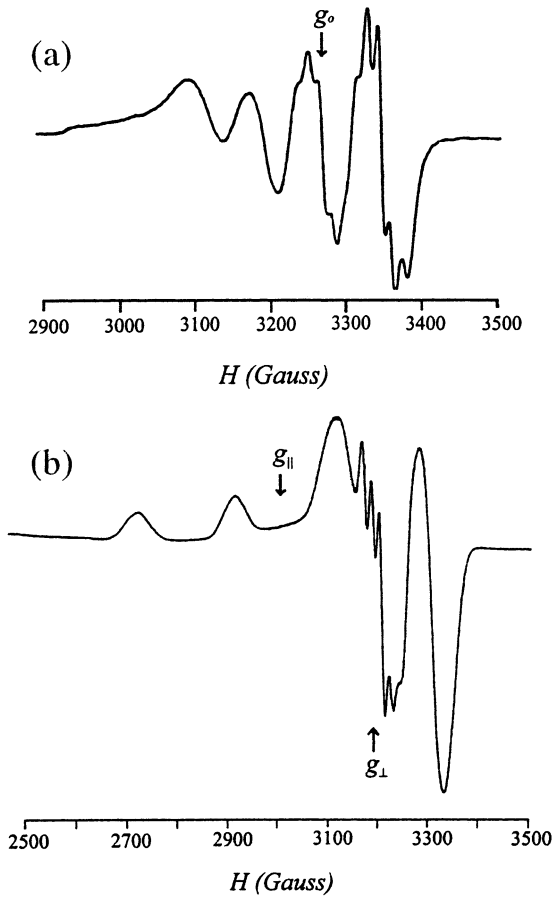

Fig. 7. ESR spectra of $[Cu(MeTtoxBF_2)]BF_4$ in 1:10 BuOH–DMF. (a) Room temperature (295 K) fluid spectrum (9.464 GHz). (b) 77 K cryogenic glass spectrum (9.147 GHz).

[66]. The lack of rhombic splitting in most of the spectra coincides with weak axial donors for the square pyramidal structures, as revealed by the X-ray crystallographic studies of $[Cu(MeTtoxH)]ClO_4$ and $[Cu(OdtoxH)]ClO_4\cdot[Cu(OdtoxH_2)](ClO_4)_2$. The large values of $|A_\parallel|$ as well as the relatively lower values of $(g_\parallel - 2)/|A_\parallel|$ (7.8–12.6) also betoken tetragonal stereochemistry in solution and most of the solids [67]. Further evidence for the persistence of tetragonal coordination over a wide temperature range in solution is provided by the similarity between the g_o values near 295 K and the $\langle g \rangle$ values at 77 K. In addition, the majority of the Cu(II) complexes exhibit nitrogen superhyperfine features in both the cryogenic glass and in the room temperature fluid spectra, indicating that the geometric relationships amongst the Cu and *N*-orbitals are preserved over this wide range of conditions. The five nitrogen superhyperfine lines observed mirror the two nitrogen donors, the coupling constants being similar to those of other tetragonal Cu(II) complexes with N/S donor sets [68]. The replacement of the oxime proton by BF_2^+ seems to have little effect on the values of $|A_\parallel|$ or $g_\perp$ as occurs in some Cu(II)–BF_2 macrocyclized oximes [3,69]. The

BF_2^+-macrocyclization does however seem to play a structural role; replacement of an H-bonded oxime linkage by a covalently bridged BF_2^+ oxime causes the donor atoms to become closer to Cu(II), and as a consequence increases the interaction between Cu(II) and the axial donor. This effect is evidenced by the large decrease in $|A_\perp|$ upon macrocyclization [70]. In $[Cu(TtoxBF_2)]BF_4$ the axial thioether sulfur is brought sufficiently close to the metal to manifest itself as a rhombic distortion in the powder spectrum (rhombicity index $R = 0.6$) [71]. The absence of rhombic features in the cryogenic spectra provides evidence for weaker axial coordination. Further evidence for a solvent coordination role is provided by the presence of a minor species at $g_\parallel \sim 2.6$ ($A_\parallel \sim 155$) in those compounds without the BF_2^+ bridge. The minor species, which is not $Cu(DMF)_n^{2+}$, is attributed to a $[Cu(L)(DMF)_x]^+$ adduct, and is also observed in the optical spectra of these complexes (vide supra).

4. Conclusions

Addition of a fifth donor atom to thioether-oxime ligands transforms the nickel(II) chelates from $S = 0$ to $S = 1$ systems. However, variation of this donor atom generally has little further effect upon the electronic properties of the Ni(II) and Cu(II) complexes. When the fifth donor atom in the ligand is thioether sulfur, the resulting nickel complexes are capable of supporting Ni(I) and Ni(III). For copper, the redox chemistry is not affected to any great extent by variation in the axial donor. BF_2^+-macrocyclization enforces the in-plane coordination in both the nickel and copper complexes. The strong in-plane effect is evident in the optical and ESR spectal data. The replacement of H^+ by BF_2^+ stabilizes the formation of M(I); this effect is most evident for the Cu(II) complexes. By understanding what role a fifth donor atom has upon the structure and reactivity of thioether oxime complexes, we hope to be able to further understand what effect ligand differences have upon the electronic, magnetic and structural properties of thioether–oxime complexes.

5. Supplementary material

Listings of atomic coordinates, anisotropic thermal parameters, F_{obs} and F_{calc}, views of unit cell contents (40 pages), as well as cif files of the structures are available upon request from the authors.

Acknowledgements

A.W.A. and M.J.P. thank Drexel University for support. We thank G.J. Gilbert, A.M. Falat and V.V. Pavlishchuk for helpful discussion as well as J.K. Murray for help with NMR experiments.

References

[1] L. Tschugaeff, Chem. Ber. 38 (1905) 2520.
[2] E. Uhlig, M. Friedrich, Z. Anorg. Allgem. Chem. 343 (1966) 299.
[3] A.W. Addison, M. Carpenter, L.K-M. Lau, M. Wicholas, Inorg. Chem. 17 (1978) 1545.
[4] A.W. Addison, C.P. Landee, R.D. Willett, M. Wicholas, Inorg. Chem. 19 (1980) 1921.
[5] A.W. Addison, B. Watts, M. Wicholas, Inorg. Chem. 23 (1984) 813.
[6] V.V. Pavlishchuk, A.W. Addison, R.J. Butcher, R.P.F. Kanters, Inorg. Chem. 33 (1994) 397.
[7] V.V. Pavlishchuk, S.V. Kolotilov, A.W. Addison, M.J. Prushan, R.J. Butcher, L.K. Thompson, Inorg. Chem. 38 (1999) 1759.
[8] M.A. Lockwood, T.J. Blubaugh, A.M. Collier, S. Lovell, Angew. Chem., Int. Ed. Engl. 38 (1999) 225.
[9] J.P. Leonard, D.P. Novotnik, R.D. Neirinckx, J. Nucl. Med. 27 (1986) 1819.
[10] J.R. Dilworth, S.J. Parrott, Chem. Soc. Rev. 27 (1998) 43.
[11] P.J. Blower, Trans. Met. Chem. (Weinheim) 23 (1998) 109.
[12] M.A. Green, Adv. Met. Med. 1 (1993) 75.
[13] M.A. Green, J. Nucl. Med. 31 (1990) 1641.
[14] E.K. John, A.J. Bott, M.A. Green, J. Pharm. Sci. 83 (1994) 587.
[15] S.S. Jurisson, J.D. Lydon, Chem. Rev. 99 (1999) 2205.
[16] W.A. Volkert, T.J. Hoffman, Chem. Rev. 99 (1999) 2269.
[17] A.A. Potekhin, T.V. Aleksandrova, V.A. Dokichev, L.V. Solov'eva, J. Org. Chem. USSR (Engl. Trans.) 26 (1990) 459.
[18] R.N. Adams, Electrochemistry at Solid Electrodes, Marcel Dekker, New York, 1969, p. 83.
[19] G.P. Lozos, B.M. Hoffman, C.G. Fronz, QCPE 11 (1974) 265.
[20] R.E. Bachman, D.F. Andretta, Inorg. Chem. 37 (1998) 5657.
[21] J.E. Parks, B.E. Wagner, R.H. Holm, Inorg. Chem. 10 (1971) 2472.
[22] A.W. Addison, T.N. Rao, J. Reedijk, J. van Rijn, G.C. Verschoor, J. Chem. Soc., Dalton Trans. (1984) 1349.
[23] S.-P. Wey, A.M. Ibrahim, M.A. Green, Polyhedron 14 (1995) 1097.
[24] J.A. Bertrand, J.H. Smith, D.G. Van Derveer, Inorg. Chem. 16 (1977) 1484.
[25] O.P. Anderson, A.B. Packard, Inorg. Chem. 18 (1979) 3064.
[26] O.P. Anderson, A.B. Packard, Inorg. Chem. 19 (1978) 2123.
[27] I.B. Liss, E.O. Schlemper, Inorg. Chem. 14 (1975) 3035.
[28] E. Bouwman, W.L. Driessen, J. Reedijk, Coord. Chem. Rev. 104 (1990) 143.
[29] G. Speier, S. Tisza, A Rockenbauer, S.R. Boone, C.G. Pierpont, Inorg. Chem. 31 (1992) 1017.
[30] T. Suzuki, T. Tsuji, T. Fukushima, S. Miyanari, T. Miyashi, Y. Sakata, T. Kouda, H. Kamiyama, J. Org. Chem. 64 (1999) 7107.
[31] M. Mascal, Chem. Commun. (1998) 303.
[32] J.A.R.P. Sarma, G.R. Desiraju, Acc. Chem. Res. 19 (1986) 222.
[33] G.R. Desiraju, Acc. Chem. Res. 24 (1991) 290.
[34] O.P. Anderson, Acta. Crystallogr., Sect. B 37 (1981) 1194.
[35] S.R. Cooper, S.C. Rawle, J.R. Hartman, E.J. Hintsa, G.A. Admans, Inorg. Chem. 27 (1988) 1209.
[36] S.M. Hart, J.C.A.. Boeyens, R.A. Hancock, Inorg. Chem. 22 (1983) 982.
[37] T.M. Donlevy, L.R. Gahan, R. Stranger, S.E. Kennedy, K.A. Byriel, C.H.L. Kennard, Inorg. Chem. 32 (1993) 6023, and refs. therein.

[38] R. Stranger, K.L. McMahon, L.R. Gahan, J.L. Bruce, T.W. Hambley, Inorg. Chem. 36 (1997) 3466.
[39] A. McAuley, S. Subramanian, Inorg. Chem. 29 (1990) 2830.
[40] D.G. Fortier, A. McAuley, Inorg. Chem. 28 (1989) 662.
[41] S. Chandrasekhar, A. McAuley, Inorg. Chem. 31 (1992) 2234.
[42] A.W. Addison, P.J. Burke, K. Henrick, T.N. Rao, E. Sinn, Inorg. Chem. 22 (1983) 3645.
[43] V.V. Pavlishchuk, P.E. Strizhak, K.B. Yatsimirskii, J. Labuda, Inorg. Chim. Acta 151 (1983) 133.
[44] N. Aoi, G.-E. Matsubayashi, T. Tanaka, Inorg. Chim. Acta 114 (1986) 25.
[45] V.V. Pavlishchuk, A.W. Addison, Inorg. Chim. Acta 298 (2000) 97.
[46] R.S. Nicholson, I. Shain, Anal. Chem. 36 (1964) 706.
[47] V.G. Levich, Physicochemical Hydrodynamic, Prentice-Hall, Englewood Cliffs, NJ, 1963.
[48] R.N. Adams, Electrochemistry at Solid Electrodes, Marcel Dekker, New York, 1969, p. 83.
[49] A. Chakravorty, Coord. Chem. Rev. 13 (1974) 1.
[50] J.G. Mohanty, R.P. Singh, A. Chakravorty, Inorg. Chem. 14 (1975) 2178.
[51] J.G. Mohanty, A. Chakravorty, Inorg. Chem. 15 (1976) 2912.
[52] A.N. Singh, R.P. Singh, J.G. Mohanty, A. Chakravorty, Inorg. Chem. 16 (1977) 2597.
[53] K. Pramanik, S. Karmaker, S.B. Choudhury, A. Chakravorty, Inorg. Chem. 36 (1997) 3562.
[54] J.-M. Bemtgen, H.-R. Gimpert, A. von Zelewsky, Inorg. Chem. 22 (1983) 3576.
[55] Y. Sulfab, N.J. Al-Shatti, Inorg. Chim. Acta 87 (1984) L23.
[56] V.V. Pavlishchuk, S.V. Kolotilov, E. Sinn, M.J. Prushan, A.W. Addison, Inorg. Chim. Acta 278 (1998) 217, and refs therein.
[57] V.V. Pavlischchuk, S.V. Kolotilov, A.W. Addison, R.J. Butcher, E. Sinn, J. Chem. Soc., Dalton Trans., submitted for publication.
[58] D.C. Boyd, G.S. Rodman, K.R. Mann, J. Am. Chem. Soc. 108 (1986) 1779.
[59] D.J. Szalda, E. Fujita, R. Sanzenbacher, H. Paulus, H. Elias, Inorg. Chem. 33 (1994) 5855.
[60] K.K. Nanda, A.W. Addison, N. Paterson, E. Sinn, L.K. Thompson, U. Sakaguchi, Inorg. Chem. 37 (1998) 1028.
[61] L. Sabatini, L. Fabbrizzi, Inorg. Chem. 18 (1979) 438.
[62] E.K. Barefield, G.M. Freeman, D.G. Van Derveer, Inorg. Chem. 25 (1986) 552.
[63] N. deVries, J. Reedijk, Inorg. Chem. 30 (1991) 3700.
[64] $G = (g_{\|} - 2)/(g_{\perp} - 2)$; B.J. Hathaway, D.E. Billing, Coord. Chem. Rev. 5 (1970) 143.
[65] J.C. Eisenstein, J. Chem. Phys. 28 (1958) 23.
[66] A.W. Addison, M. Palaniandavar, Abstr. Pap., Am. Chem. Soc. (1984) 188th INORG 068.
[67] K.K. Nanda, A.W. Addison, R.J. Butcher, M.R. McDevitt, T.N. Rao, E. Sinn, Inorg. Chem. 36 (1997) 134.
[68] G.D. Shields, S. Christiano, R.D. Bereman, J. Inorg. Nucl. Chem. 40 (1978) 1953.
[69] H. Yokoi, T. Kishi, Chem. Lett. (1979) 749.
[70] I. Adato, I. Eliezer, J. Chem. Phys. 54 (1971) 1472.
[71] $R = (g_2 - g_1)/(g_3 - g_2)$; N.J. Ray, L. Hulett, R. Sheahan, B.J. Hathaway, J. Chem. Soc., Dalton Trans. (1981) 1463.